Universiteit
Leiden
The Netherlands

Barrier properties of human skin equivalents : rising to the surface

Thakoersing, V.S.

Citation
Thakoersing, V. S. (2012, June 7). *Barrier properties of human skin equivalents : rising to the surface*. Retrieved from https://hdl.handle.net/1887/19056

Version:	Corrected Publisher's Version
License:	Licence agreement concerning inclusion of doctoral thesis in the Institutional Repository of the University of Leiden
Downloaded from:	https://hdl.handle.net/1887/19056

Note: To cite this publication please use the final published version (if applicable).

Cover Page

Universiteit Leiden

The handle http://hdl.handle.net/1887/19056 holds various files of this Leiden University dissertation.

Author: Thakoersing, Varsha Sakina
Title: Barrier properties of human skin equivalents : rising to the surface
Date: 2012-06-07

3

UNRAVELING BARRIER PROPERTIES OF THREE DIFFERENT IN-HOUSE HUMAN SKIN EQUIVALENTS

Varsha S. Thakoersing[1], Gerrit S. Gooris[1], Aat Mulder[1], Marion Rietveld[2], Abdoelwaheb El Ghalbzouri[2], Joke A. Bouwstra[1]

[1] Leiden/Amsterdam Center for Drug Research, Department of Drug Delivery Technology, Gorlaeus Laboratories, Leiden University, 2333 CC Leiden, The Netherlands.

[2] Leiden University Medical Center, Department of Dermatology, Leiden University, 2333 ZA Leiden, The Netherlands

Adapted from Tissue Engineering Part C Methods. 2012 Jan;18(1):1-11.

ABSTRACT

Human skin equivalents (HSEs) are three dimensional culture models that are used as a model for native human skin. In this study the barrier properties of two novel HSEs, the Fibroblast Derived matrix Model (FDM) and the Leiden Epidermal Model (LEM), were compared with the Full Thickness collagen Model (FTM) and human skin. As the main skin barrier is located in the lipid regions of the upper layer of the skin, the stratum corneum (SC), we investigated the epidermal morphology, expression of differentiation markers, SC permeability, lipid composition and lipid organization of all HSEs and native human skin. Our results demonstrate that the barrier function of the FDM and LEM improved compared to that of the FTM, but all HSEs are more permeable than human skin. Furthermore, the FDM and LEM have a relatively lower free fatty acid content than the FTM and human skin. Several similarities between the FDM, LEM and FTM were observed: 1) the morphology and the expression of the investigated differentiation markers were similar to that observed in native human skin, except for the observed expression of keratin 16 and premature expression of involucrin which were detected in all HSEs 2) the lipids in the SC of all HSEs were arranged in lipid lamellae, similar to human skin, but show an increase in the number of lipid lamellae in the intercellular regions, and 3) the SC lipids of all HSEs show a less densely packed lateral lipid organization compared to human SC. These findings indicate that the HSEs mimic many aspects of native human skin, but differ in their barrier properties.

INTRODUCTION

The skin provides a possible delivery route of active compounds either to the various skin layers or to the systemic circulation. Penetration studies with preferably *ex vivo* human skin can be performed to investigate whether compounds show promise for dermal or transdermal application. However, the use of *ex-vivo* skin is not always possible due to practical issues. The use of human skin equivalents (HSEs) can therefore provide an alternative for native human skin. HSEs have already been used for various applications such as the treatment of burn wounds [1-3], cutaneous irritation and toxicity testing of substances [4-7] and the generation of diseased skin models [8-11]. Many HSEs have a fairly similar morphology and a comparable expression of several differentiation markers as native human skin [12-17]. However, when HSEs are evaluated for their resemblance to native human skin it is also important to examine their barrier properties. The stratum corneum (SC), which is the outermost layer of the epidermis, forms the first and main barrier of the skin against penetration of exogenous substances. The SC consists of protein rich dead cells that are embedded in a lipid matrix. As the lipids form a continuous pathway in the SC, the lipid domains play a crucial role in the barrier properties of the skin. The SC consists of three main lipid classes, which are cholesterol, free fatty acids and ceramides. These lipids form two lamellar phases with a repeat distance of approximately 13 nm or 6 nm, referred to as the long periodicity phase (LPP) and short periodicity phase (SPP), respectively (see figure 1A) [18-21]. Besides the lamellar organization the lateral packing is also important for a proper barrier function of the SC. The lateral packing discloses information about the density of the lipids within the lipid lamellae. In native human skin, the majority of the SC lipids within the lipid lamellae form crystalline phases. A large fraction of lipids forms the very dense orthorhombic packing, but a small population of lipids also forms the less dense hexagonal or even liquid packing [21-24]. A schematic presentation of these crystalline and liquid phases is shown in figure 1A.

When HSEs are used for *in vitro* permeation studies they generally show a higher permeability compared to human skin, indicative of an impaired barrier function [25-32]. Several studies have been performed in which the barrier properties of various HSEs were examined. However, these studies mainly focused on the SC lipid composition. They showed that HSEs are prone to have a reduced free fatty acid content [14, 25, 33-36]. The few studies in which the SC lateral and lamellar organization of some HSEs have been examined were performed more than a decade ago. These studies mostly showed a predominantly hexagonal packing [34, 37] in HSEs and the presence of the LPP [33, 35, 37]. However, not all models showed a continuous presence of lipid lamellae in the SC or the presence of the LPP [14].

In this study we evaluated the barrier properties of two recently developed HSEs - the fibroblasts derived matrix model (FDM) and the Leiden Epidermal Model (LEM) and compared their barrier properties, which have not been investigated before, with the Full Thickness collagen Model (FTM). The FDM model consists of a dermal compartment based on a human fibroblast-derived matrix [38], while the dermal equivalent of FTM consists of rat-tail collagen populated with fibroblasts [39]. The LEM is an epidermal equivalent generated on an inert filter. To evaluate to which extent these three HSEs mimic the barrier properties of native human skin and to assess their suitability for e.g. permeability testing, we have examined their SC lipid composition, lipid organization and permeability and compared that with native human skin.

Figure 1. A: The SC lipids are organized into lipid layers (i.e. lamellae) stacked on top of each other, referred to as the lamellar phase. The most important parameter to characterize this phase is the repeat distance (d). This is distance over which the molecular structure is repeated. In native human SC the lipids are organized into two lamellar phases, the long periodicity phase (LPP) and the short periodicity phase (SPP) with repeat distances of around 13 and 6 nm, respectively. In the plane perpendicular to

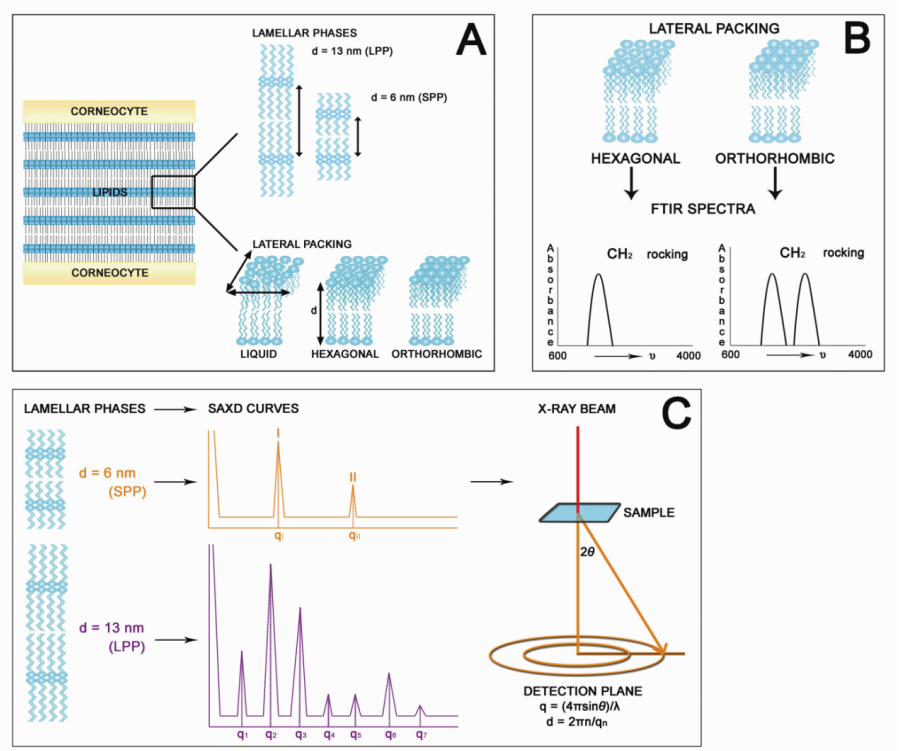

the direction of the lamellar repeats the lipid organization is referred to as the lateral packing. The lateral packing is liquid, hexagonal or orthorhombic. The liquid packing is the least dense packing, while the orthorhombic packing has the highest density of lipids. B: Due to atom bond vibrations, molecules absorb infrared light at characteristic wavenumbers. This absorption provides information about inter- and intramolecular interactions. The CH_2 rocking vibration of the hydrocarbon chains provides information about the lateral packing of the lipids. A single contour at around 719 cm^{-1} is observed when lipids are arranged in a hexagonal packing, while two peaks (around 719 and 730 cm^{-1}) are characteristic for an orthorhombic packing. C: X-rays that pass a sample are scattered by the sample, resulting in a characteristic diffraction pattern. The scattered intensity is plotted as a function of q, the scattering vector. q is defined as $4\pi\sin\theta/\lambda$, in which θ is the scattering angle and λ is the wavelength of the X-rays. In case of a lamellar phase the diffraction peaks in the pattern are all at the same interpeak distance. The position of the peaks (q_1, q_2, q_3,…,q_n, n being the order of the peak) are related to the repeat distance of a lamellar phase by $d=2\pi n/q_n$. As this is a reciprocal relationship, the 1st and 2nd order peak of the SPP is located at higher q-values that that of the LPP.

MATERIALS AND METHODS

Cell culture

Normal human keratinocytes (NHKs) and human dermal fibroblasts were obtained from adult donors undergoing mammary or abdomen surgery and were established as described previously [39]. NHKs used to create HSEs with only an epidermal compartment were generated with the Dermalife K medium complete kit (Lifeline Cell Technology, Walkersville, MD). The NHKs were grown to a maximum confluency of 80% before trypsin digestion. First and second passage NHKs were used to generate HSEs.

Dermal equivalents

Collagen-type I containing dermal equivalents: collagen-type I containing dermal equivalents were generated as described earlier [39]. Collagen was isolated from rat tails and dissolved in 0.1% acetic acid to a concentration of 4 mg/mL. This solution was mixed at 4ºC with Hank's Buffered Salt Solution (HBSS) (Invitrogen, Leek, The Netherlands), 0.1% acetic acid, 1M NaOH and fetal bovine serum (FBS) (Hyclone, Logan, UT) to obtain a final collagen concentration of 1 mg/mL. One mL of the mixture was pipetted into a filter insert (Corning transwell cell culture inserts, membrane diameter 24 mm, pore size 3 μm, Corning Life Sciences, Amsterdam, The Netherlands) and was allowed to polymerize for 15 minutes at 37ºC. Hereafter, a 2 mg/mL collagen solution was prepared at 4ºC with the 4 mg/mL collagen stock solution, HBSS, 0.1% acetic acid, 1M NaOH and a fibroblasts containing FBS solution (final fibroblast cell density of $0.4x10^5$ cells/mL collagen solution). Three mL of this mixture was pipetted onto the previously polymerized collagen layer. The new collagen layer was placed at 37ºC to polymerize. After the final polymerization step the dermal equivalents were placed in a 6-well deep-well plate (Organogensis, Canton, MA) and submerged in medium consisting of Dulbecco's Modified Eagle Medium (DMEM; Invitrogen, Leek, The Netherlands), 5% FBS, 1% penicillin/streptomycin (Sigma) and fresh

supplementation with 45 mM vitamin C (Sigma). The medium was refreshed twice a week.

Fully human dermal equivalents: the dermal compartment of the FDMs were generated as described before [38]. Briefly, $0.4x10^6$ fibroblasts were seeded onto filter inserts (Corning Transwell culture inserts, membrane diameter 24 mm, pore size 0.4 μm; Corning Life Sciences, Amsterdam, The Netherlands). The fibroblasts were nourished with the medium described for the collagen type I containing dermal equivalents for 3 weeks, during which the cells generated a dermal matrix. The medium was refreshed twice a week.

Generation of human skin equivalents (HSEs)

HSEs generated on collagen dermal equivalents referred to as Full Thickness collagen Model (FTM): One week after generation of the collagen dermal equivalents, $0.5x10^6$ NHKs were seeded onto each dermal equivalent. The HSEs were kept submerged for 2 or 3 days with a 3:1 mixture of DMEM and Ham's F12 medium supplemented with 5% FBS, 1% penicillin/streptomycin solution, 0.5 μM hydrocortisone, 1 μM isoproterenol and 0.5 μg/mL insulin. Hereafter, the HSEs were kept submerged for an additional 2 days with medium in which the FBS was reduced to 1% and the medium was additionally supplemented with 0.053 μM selenious acid (Johnson Matthey, Maastricht, The Netherlands), 10 mM L-serine (Sigma), 10 μM L-carnitine (Sigma), 1 μM α-tocopherol acetate (Sigma), 25 mM vitamin C and a lipid mixture of 3.5 μM arachidonic acid (Sigma), 30 μM linoleic acid (Sigma) and 25 μM palmitic acid (Sigma). This medium is referred to as K^1-medium. The HSEs were subsequently lifted to the air-liquid interface. For the remaining culture period the HSEs were fed with a medium similar to K^1-medium except that the FBS was omitted and the arachidonic acid concentration was increased to 7 μM. The culture medium was refreshed twice a week. The HSEs were grown for 16 days after seeding the NHKs.

HSEs generated on fully human dermal equivalents referred to as Fibroblast Derived matrix Model (FDM): three weeks after seeding fibroblasts onto filter inserts, $0.5x10^6$ NHKs were seeded onto each dermal equivalent. The HSEs were further cultured as described for the FTMs.

HSEs generated on inert filter, referred to as Leiden Epidermal Model (LEM): LEM was generated with minor modifications of the culture conditions described by El Ghalbzouri *et al.* [7]. NHKs (0.2 x 10^6 cells/filter) were seeded directly onto cell culture inserts (Corning Transwell cell culture inserts, membrane diameter 12 mm, pore size 0.4 μm; Corning Life Sciences, Amsterdam, The Netherlands) and were kept submerged in Dermalife medium until confluency. Hereafter the HSEs were kept submerged in CnT medium (CellnTec, Bern, Switzerland), which was supplemented according to the manufacturer's protocol, and 1% penicillin/streptomycin solution (Sigma, Zwijdrecht, The Netherlands), 1 μM α-tocopherol acetate (Sigma), 25 mM vitamin C (Sigma) and a lipid mixture of 7 μM arachidonic acid (Sigma), 30 μM linoleic acid (Sigma) and 25 μM palmitic acid (Sigma). After two days the HSEs were lifted to the air-liquid interface. The LEMs were cultured at the air-liquid interface for 12 days before harvesting.

Morphology and immunohistochemistry

Harvested HSEs were fixed in 4% (w/v) paraformaldehyde (Lommerse Pharma, Oss, The Netherlands), dehydrated and subsequently embedded in paraffin. 5 μm sections were cut, deparaffinized, rehydrated and stained with haematoxylin and eosin for analysis by light microscopy. Immunohistochemical staining of keratin 10, keratin 16, filaggrin, loricrin and involucrin was performed on paraffin sections as described before [39, 40]. Immunofluorescent staining of aquaporin 3 (Santa Cruz Biotechnology, Santa Cruz, CA) was performed on frozen sections that were fixed in acetone. The aquaporin 3 antibody (1:50 dilution) was applied for 60 min followed by incubation with donkey anti-goat FITC-labelled secondary antibody (1:100 dilution) (Jackson ImmunoResearch Europe, Suffolk, UK) for 60 min.

Sections were enclosed with Vectashield mounting medium with DAPI (Vector Laboratories, Peterborough, UK).

Stratum corneum isolation and diffusion study

The SC of HSEs and human skin was isolated as described by De Jager *et al.* [41]. The diffusion study with benzocaine and further analysis with HPLC, to deteremine the flux of benzocaine through each SC sample, was performed as described earlier [41] with modification of the mobile phase to methanol:water (50:50 v/v). The diffusion study was performed with at least 4 SC sheets from each HSE type or human skin.

Lipid extraction and analysis

SC samples were consecutively extracted according to a modified Bligh and Dyer procedure with the addition of 0.25M KCl to extract polar lipids as described before [40, 42]. The extracted lipids were analyzed by means of one-dimensional high performance thin layer chromatography (HPTLC) as described before [40]. The ceramides are named according to the nomenclature defined by Motta *et al.* [43] and Masukawa *et al.* [44]. Briefly, ceramides with a sphingosine (S), phytosphingosine (P) or 6-hydroxysphingosine (H) are linked via an amide to a fatty acid chain, which can either be an estrified ω-hydroxy (EO), α-hydroxy (A) or non-hydroxy (N) fatty acid.

Fourier transform infrared spectroscopy (FTIR) and small angle x-ray diffraction (SAXD)

The SC samples for FTIR and SAXD measurements were hydrated at room temperature for 24 hours over a 27% (w/v) NaBr solution. The hydrated SC samples for FTIR were measured as described before [45]. The phase transitions of the SC lateral lipid organization were examined as a function of temperature from

0ºC to 90ºC with a heating rate of 1ºC/4 min. At least 3 SC sheets of each HSE type or human SC were measured.

SAXD measurements were performed at the European Synchrotron Radiation Facility (ESRF) in Grenoble as described before [45]. SC samples were clamped in specially designed holders and measured at room temperature for 10 minutes. The scattered intensity was measured as function of q. q is defined as $q= 4\pi\sin\theta/\lambda$, in which λ is the wavelength of the X-rays and θ the scattering angle. Repeat distances of lamellar phases are calculated from the peak positions; $d= 2\pi n/q_n$, in which n is the order of the peak and q_n its position. At least 2 samples of each HSE type or human SC were measured. A schematic overview of the FTIR and SAXD measurements is depicted in figure 1B and C, respectively.

Transmission electron microscopy (TEM)

HSEs were fixed in 2% paraformaldehyde-2.5% glutaraldehyde in 0.1M sodium cacodylate buffer (pH 7.4) followed by a first post-fixation in 1% osmium tetroxide in cacodylate buffer and a second post-fixation in 0.5% ruthenium tetroxide. Hereafter the samples were dehydrated in 70% ethanol and subsequently processed in a series of 70% ethanol/epoxy resin LX112 (LADD Research Industries, Williston, VT) dilutions and finally in 100% epoxy resin. Ultrathin sections were stained with uranyl-acetate and lead hydroxide and visualized with a Fei Tecnai 12 Twin (Spirit) (Fei Europa, Eindhoven, The Netherlands) electron microscope. At least 2 cultures per HSE type were examined and at least 20 images per culture were made.

Figure 2. Haematoxylin and eosin (HE) and immunohistochemical staining of the expression pattern of keratin 10, keratin 16, filaggrin, loricrin, involucrin and aquaporin 3 (green pattern in the image) in FDM, LEM, FTM and native human skin are shown. Scale bar represents 50 μm.

RESULTS

The morphology and differentiation process show similarities between HSEs and native human skin

FDM, LEM and FTM show a fairly similar morphology and expression of the investigated differentiation markers, except for two markers which are indicative of an activated epithelium, when compared to human skin (figure 2). All HSEs show the presence of all epidermal strata, including a SC. The keratinocytes become flat and elongated as they migrate and differentiate from the basal layer towards the upper spinous and granular layer. In the latter layer keratohyalin granules can be detected. Occasionally the stratum granulosum in the LEM consisted of more cell layers than observed for the FDM, FTM and human skin. Furthermore, all HSEs show similar expression of the early differentiation marker keratin 10, the water/glycerol transporting channel aquaporin 3 and the two terminal differentiation markers filaggrin and loricrin as human skin (figure 2). Filaggrin and loricrin are only detected in the stratum granulosum, while keratin 10 is detected in the suprabasal layers and aquaporin 3 in the cell membranes of all cells in the viable epidermis. In native human skin involucrin expression is confined to the granular layer and keratin 16 expression is absent. In all HSEs however, involucrin and keratin 16 are expressed throughout the suprabasal layers of the viable epidermis, which are signs of an activated epithelium.

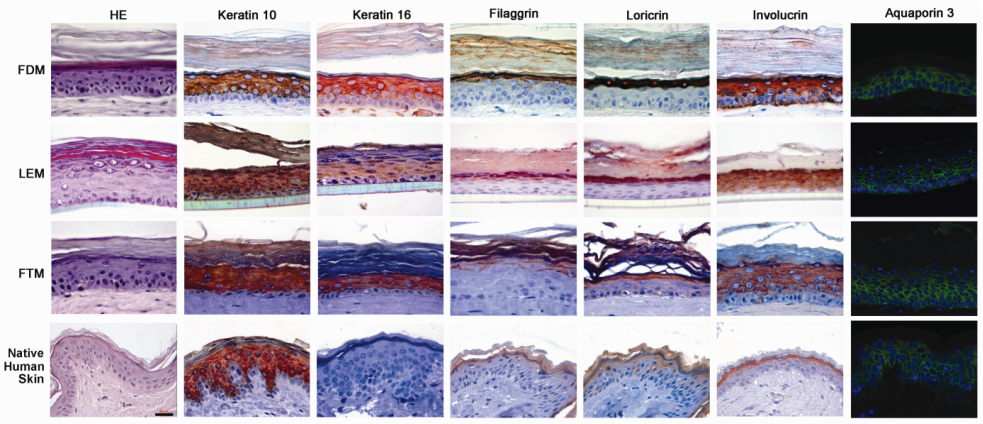

The SC of the HSEs contains all barrier lipid classes that are present in human skin

The three lipid classes present in human SC, namely cholesterol, free fatty acids and ceramides, are also present in the SC of the HSEs (figure 3). In addition, the HSEs show the presence of all ceramide subclasses that are present in native human SC. However, some differences can be noticed in the relative abundance of free fatty acids and ceramides when the different lipid profiles are compared. The FDM and LEM exhibit a relatively lower level of free fatty acids compared to human SC. However, the lipid profile of the FTM indicates that in this model the free fatty acid level is higher than in the LEM and FDM and appears to be comparable to native human SC. Furthermore, all HSEs seem to have a higher relative content of ceramides EOS and EOP. The LEM and FTM have an additional ceramide subclass, with a retention factor between that of ceramide NP and AS (figure 3; indicated by *), that is not present in the FDM or human SC.

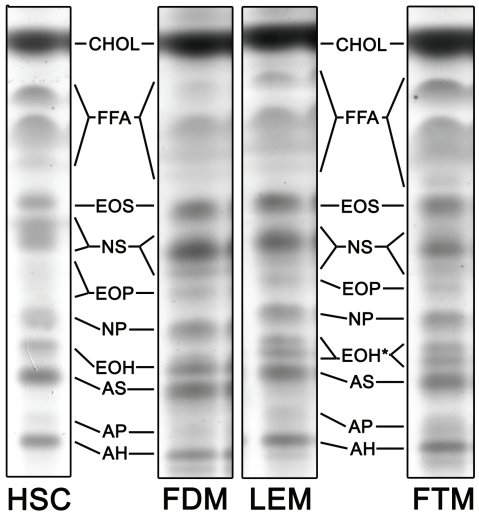

Figure 3. The SC barrier lipid profile of each HSE and human SC are shown. The HSEs contain all lipid classes that are also present in human SC, namely cholesterol (CHOL), free fatty acids (FFA) and ceramides. The FTM and LEM show the presence of an additional ceramide subclass (*) that is not detected in human SC or the FDM.

Permeability assessment of HSEs and native human skin

To investigate the barrier function of the HSEs a diffusion study was performed. Figure 4 shows the diffusion profile of benzocaine through the SC of the three HSEs and native human skin. These results show that the FDM and LEM have an improved barrier function compared to FTM. The calculated steady-state flux (figure 4) indicates that the SC of the FDM and LEM is approximately 3 times more permeable than native human SC, whereas the SC of FTM is about 5 times more permeable. The lag-time of the benzocaine flux through the SC of the FDM and FTM is slightly lower compared to native human SC.

	Human SC	FDM	LEM	FTM
$Flux_{ss}$ ($\mu g/hr/cm^2$)	13.6 ± 3.5	44.5 ± 4.6	47.0 ± 5.8	65.8 ± 4.0
T_{LAG} (hr)	0.5 ± 0.2	0.2 ± 0.1	0.6 ± 0.4	0.2 ± 0.0

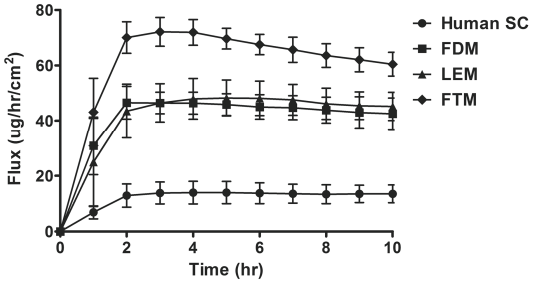

Figure 4. Benzocaine was used as a model drug to investigate the permeability of the three HSEs and human SC. The data represent the mean and standard deviation of at least 4 measurements. The estimated steady-state flux ($Flux_{ss}$) and lag-time (T_{lag}) of benzocaine through the SC of human skin and the three HSEs are also shown.

The lateral packing in the SC of the three HSEs differs from human SC

The lateral packing in the SC of the three HSEs and human skin were examined using FTIR. The lateral packing can be determined by monitoring the rocking bands in an FTIR spectrum. When lipids are in a crystalline orthorhombic packing the CH_2 rocking band consists of two vibrations at 719 cm^{-1} and 730 cm^{-1}, while a crystalline hexagonal lateral packing results in a single vibration at 719 cm^{-1}. An example of the thermotropic response of the CH_2 rocking band as a function of temperature in the FDM, LEM, FTM and native human SC are shown in figure 5. In general the HSEs show a strong peak at 719 cm^{-1} and a smaller peak at 730 cm^{-1} at lower temperatures. This indicates that in that temperature region the lipids in the SC mainly form a hexagonal lateral packing and a small population of lipids forms an orthorhombic packing. In human SC the high intensity of the 730 cm^{-1} peak indicates an abundant formation of the orthorhombic lateral packing. The temperature at which the orthorhombic packing transforms into the hexagonal packing, indicated by the disappearance of the 730 cm^{-1} peak, varies between each HSE type and also between samples of the same HSE type and native human skin.

Figure 5. Examples of the lateral lipid organization as a funtion of temperature are shown for the FDM, LEM, FTM and native human SC (HSC) (a, b, c and d, respectively). At lower temperatures the lipids in the FDM, LEM and FTM mainly form a hexagonal lateral packing (strong vibrations at 719 cm^{-1}) and a minor population of lipids forms an orthorhombic packing (weak vibrations at 730 cm^{-1}). The transition to a hexagonal packing, indicated by the disappearance of the 730 cm^{-1} peak, occurs at approximately 24ºC, 30ºC and 26ºC in the FDM, LEM and FTM, respectively. In human SC (d) a doublet is observed with a high intensity peak at 730 cm^{-1} , representing a dominant orthorhombic packing. The orthorhombic packing disappears between 28ºC to 40ºC. At higher temperatures only a singlet is observed signifying a hexagonal packing. Figure e shows the transition from a hexagonal to a liquid phase detected by the symmetric stretching vibrations. The liquid phase is formed between 56-84ºC in the HSEs and between 66-86ºC in human SC.

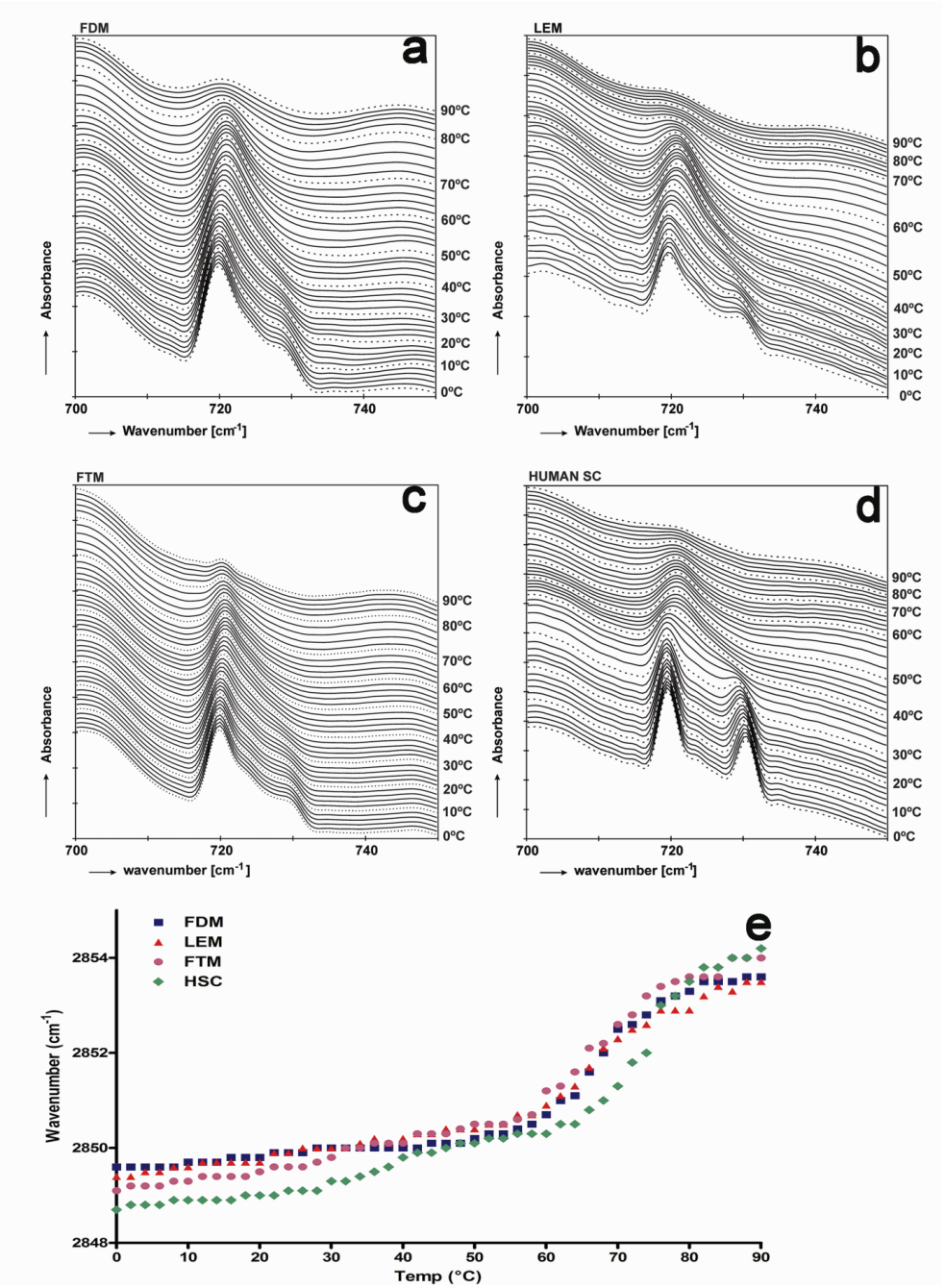
FDM
a
LEM
b
FTM
c
HUMAN SC
d
Absorbance
Wavenumber [cm-1]
wavenumber [cm-1]
90°C
80°C
70°C
60°C
50°C
40°C
30°C
20°C
10°C
0°C
700
720
740
e
FDM
LEM
FTM
HSC
Wavenumber (cm-1)
Temp (°C)
2854
2852
2850
2848
0
10
20
30
40
50
60
70
80
90

In FDM the orthorhombic packing disappears at a temperature that varies between 8-24ºC, in FTM between 14-26ºC, in LEM between 24-30ºC and in native human SC between 40-50ºC. At which temperature the lipids finally form a liquid phase can be determined from the CH_2 symmetric stretching mode, which provides information about the conformational disorder. In a crystalline phase (hexagonal or orthorhombic packing) the conformational disorder is low resulting in symmetric stretching frequencies below 2850 cm^{-1}. In a liquid phase, the conformational disordering is high resulting in symmetric stretching vibrations of around 2852-2854 cm^{-1}. The transition from a crystalline to a conformational disordered liquid phase can therefore be distinguished by a steep increase in wavenumber. In human SC the CH_2 symmetric stretching is around 2848.5 cm^{-1} at 0ºC and increases slightly when the temperature is raised. Between 30-40ºC there is a steeper shift, indicating the orthorhombic to hexagonal phase transition. A further increase to 66ºC results in a gradual shift in wavenumber. At 66ºC a steep shift is noticed from 2850.9 cm^{-1} to 2854.0 cm^{-1} at 86ºC, which corresponds to the formation of a liquid phase (figure 5e). When focussing on the HSEs, between 0ºC and 56ºC a gradual increase in wavenumber from around 2849.5 to 2850.4 cm^{-1} is observed. The symmetric stretching is located at higher wavenumbers than observed for native human SC. Above 56ºC a steep increase in wavenumber is observed to 2853.2 – 2853.6 cm^{-1} at 82-84ºC (figure 5e) demonstrating the formation of the liquid phase. The liquid phase is formed at a lower temperature in the SC of the HSEs compared to human SC.

The SC intercellular lipid regions of HSEs are composed of more lipid lamellae than native human skin

Transmission electron microscopy images taken at the stratum garnulosum/SC interface show the lamellar body extrusion process in the HSEs similarly as observed in native human skin (figure 6a, c, e and g). The extruded lipids are neatly arranged into lipid lamellae (figure 6b, d, f and h), which is characteristic for the SC

lipid organization. When compared to human SC it is evident that the HSEs contain a higher number of lipid lamellae between corneocytes. This finding indicates that the intercellular lipid regions in the SC of the HSEs are more pronounced than in human SC.

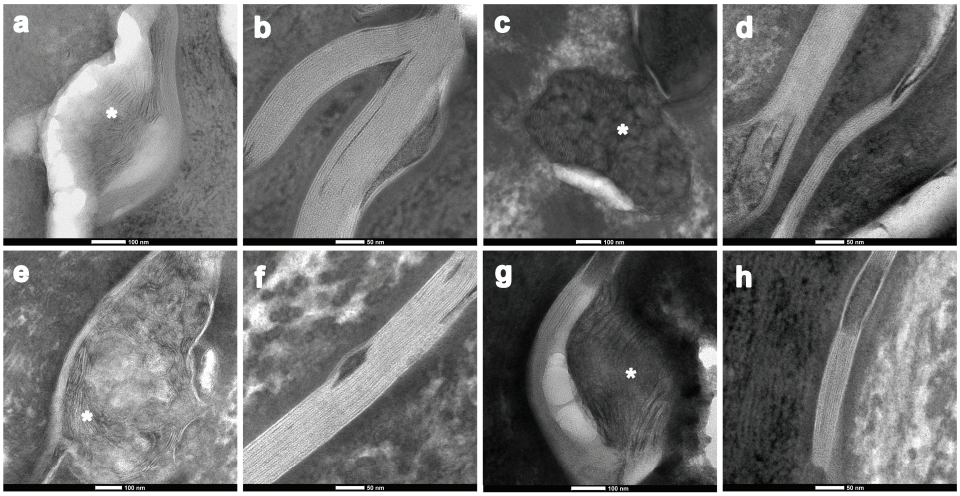

Figure 6. The lipid lamellae in the SC of the three HSEs and human skin were visualized with TEM. Representative images of each HSE and human SC are shown. Figure a, c, e and g represent the lamellar extrusion process in FDM, LEM, FTM and native human skin, respectively (scale bar represents 100 nm). Figure b, d, f and h show the formed lipid lamellae in the SC of FDM, LEM, FTM and native human skin, respectively (scale bar represent 50 nm). *= lamellar body.

The SC lipids in HSEs form the LPP similar to native human skin

The observed lamellar organization in the SC of the three HSEs and native human skin (figure 6) was also investigated by SAXD. The SAXD profiles of all three HSEs show the presence of three sharp diffraction peaks (figure 7; referred to as 1, 2 and 3) that can be attributed to the LPP with a corresponding repeat distance varying between 11.8 - 12.6 nm, 12.6 - 12.8 nm and 11.6 - 12.5 nm for the FDM, LEM and FTM, respectively. However, no peaks are observed that can be

attributed to the SPP. The presence of crystalline cholesterol can also be detected in the diffraction profiles of all three HSEs (figure 7; indicated by *).

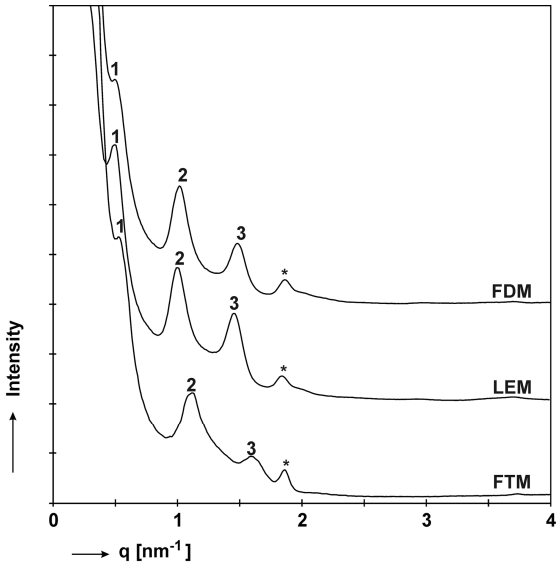

Figure 7. A representative SAXD profile of each HSE type is shown. The 1st, 2nd and 3rd order diffraction peaks of the LPP (indicated by 1, 2 and 3, respectively) are located at q= 0.50, q= 1.01 and q= 1.48 nm^{-1} for the FDM, corresponding to a repeat distance of 12.6 nm. For the LEM the various orders of the LPP are located at q= 0.50, q= 1.00 and q= 1.46 nm^{-1}, indicating a repeat distance of 12.7 nm. For the FTM the various orders of the LPP are located at q= 0.52, q= 1.01 and q= 1.59 nm^{-1}, which corresponds to a repeat distance of 11.7 nm. At q= 1.84 nm^{-1} a reflection is detected in all profiles demonstrating the presence of phase separated crystalline cholesterol (indicated by *).

Discussion

In order to obtain a suitable replacement of native human skin for penetration studies or for safety testing of compounds, we compared two novel in-house skin models with FTM and native human skin and evaluated their SC barrier properties. An overview of the SC barrier properties of the three HSEs and human skin is provided in table 1. Both FDM and LEM show an improved SC barrier function compared to FTM, indicated by the higher flux of benzocaine through the SC of

FTM. Although the SC barrier function of the novel HSEs has improved and mimics more closely the SC barrier function of native human skin, it is still reduced compared to native human skin. A reduced SC barrier function has also been reported for other HSE types, including the commercially available models Epiderm (Mattek), Episkin and SkinEthic [25-32]. As the lipid organization is a crucial determinant for the SC barrier function, we examined the lamellar phases and the lateral packing in all three HSEs and compared that to native human SC.

Table 1. Overview SC barrier properties human skin *vs* HSEs

	Lamellar Packing (RT)	***Lateral Packing (RT)***	***SC Lipid Composition***	***Benzocaine $Flux_{ss}$ ($\mu g/hr/cm^2$)***
Native HS	LPP + SPP	Orthorhombic	CHOL, FFA, CERs	13.6 ± 3.5
FDM	LPP	Hexagonal	CHOL, FFA ↓, CERs EOS and EOP ↑	44.5 ± 4.6
LEM	LPP	Hexagonal	CHOL, FFA ↓, CERs EOS and EOP ↑	47.0 ± 5.8
FTM	LPP	Hexagonal	CHOL, FFA, CERs EOS and EOP ↑	65.8 ± 4.0

An overview of the SC barrier properties of native human skin (HS) and SC of FDM, LEM and FTM are shown. RT = room temperature, CHOL= cholesterol, FFA= free fatty acid, CER= ceramides, $Flux_{ss}$= steady state flux, arrows indicate an increase (↑) or decrease (↓) compared to native human SC.

Morphology and expression of differentiation markers

All three HSEs show a similar morphology and expression of several differentiation markers as native human skin, except for the expression of involucrin and keratin 16, which were detected throughout the suprabasal viable epidermis in all three HSEs. The observed expression of keratin 16 and the early

start of the terminal differentiation program indicated by the premature expression of involucrin might be explained by an over-activated cell differentiation due to compounds or possible growth factors present in the commercial culture media, or by the number of fibroblasts present in the dermal matrices [15, 16]. The over-activated differentiation programme observed in the HSEs may have an effect on the barrier properties of the HSEs. An altered expression of differentiation markers has also been observed in the commercially available models [12]. These models showed a fully differentiated epidermis and an expression pattern for keratin 10 and loricrin that is mainly similar to native human skin. However, all commercial skin models showed a premature expression of involucrin compared to native human skin, indicating that homeostasis was not yet achieved in these models. Cheng *et al.* [46] and El Ghalbzouri *et al.*[13] showed that it is possible to generate HSEs that do not demonstrate the premature expression of involucrin and/or the presence of activation associated markers like keratin 6, 16 and 17. However, it still remains to be investigated whether a normalized involucrin expression or the absence of activation associated markers lead to improved SC barrier properties. Previous studies have shown that the SC of FTM is less hydrated than human SC [39]. The similar expression of the water/glycerol transporting channel aquaporin 3 in the HSEs and native human skin indicates that the reduced SC hydration in FTM is not caused by the absence of aquaporin 3.

Lamellar organization

Our results demonstrate that in all three HSEs the LPP is formed, similar to native human skin [21], while there is no indication of the formation of the SPP. The latter is present in native human SC. Previous studies demonstrated that the presence of acylceramides, such as acylceramides EOS and EOP, induce the formation of the LPP [22]. These ceramides are present in relatively higher amounts in the HSEs compared to native human skin and therefore may account for the abundant presence of the LPP. However, this most probably does not contribute to the

reduced skin barrier function of the HSEs, as the LPP plays a more prominent role in the skin barrier function than the SPP [41]. In 2000 Ponec *et al.*[14] reported the lamellar organization of the EpiSkin and EpiDerm penetration models. In the EpiDerm model an LPP with a repeat distance of 12 nm was clearly detected, while the EpiSkin model showed signs of a poor lamellar organization. Although both the EpiDerm and Episkin models had approximately the same relative amount of ceramide EOS as native human skin, ceramides EOP, AS, AP and AH were minimally present or even absent [6, 14].

When we examine the EM images, the SC of the HSEs seem to contain a larger number of lipid lamellae than observed for human SC. The sharp peaks observed in the SAXD profiles clearly indicate that the mean number of lipid lamellae between the cells is increased in the SC of the HSEs compared to native human SC; the width of half maximum is proportional to 1/N, in which N is the number of lamellae in a stack [47]. Since the penetration of substances through the SC mainly proceeds via the lipid domains we hypothesize that the increased number of lipid layers in the HSEs form wider intercellular 'channels' for compound penetration, which may attribute to the impaired skin barrier function of the HSEs. The SC intercellular lipid domains of the commercially available skin models have also been examined by EM [14]. All models showed the presence of lipid lamellae, however, this was not continuously observed throughout the SC in all models. Additionally, some EpiSkin models showed an incomplete lamellar body extrusion process.

Lateral packing

When focussing on the lateral packing, HSEs have a hexagonal packing rather than an orthorhombic packing that is present in native human SC. Previous studies [18] have shown that long-chain free fatty acids (e.g. free fatty acids with a chain length of 24 or 26 carbon atoms), promote the formation of an orthorhombic packing in SC lipid mixtures, while a reduction in these fatty acids results in a more prominent

formation of the hexagonal packing. These findings suggest that a reduced free fatty acid content in the FDM and LEM may contribute to the absence of an orthorhombic packing. The free fatty acid level in FTM mimics the free fatty acid content of human SC more closely, but nonetheless the lipids also form a hexagonal packing. Therefore other factors also play a role, such as a possible reduction in the chain length of the free fatty acids or the presence of unsaturated fatty acids. Based on previous studies, both of these aberrations are expected to reduce the formation of the orthorhombic packing [48]. To gain more insight in this phenomenon the free fatty acid chain length distribution and degree of saturation in the HSEs will be subject of future studies. Whether the hexagonal packing contributes to the increased permeability for substances like benzocaine is not yet clear. Although the hexagonal packing is less dense than the orthorhombic packing, very recently no difference in the benzoic acid permeability was observed between SC lipid membranes forming either a hexagonal packing or an orthorhombic packing [49].

Formation of a liquid phase

The higher degree of conformational disorder observed for the HSEs at 32ºC, which is the normal skin temperature, suggests an increased proportion of gauche conformations in the alkyl chains of the fatty acids or ceramides in the SC of HSEs compared to human SC. This may signify that relatively more lipids may already be in the liquid phase at 32ºC compared to lipids in the SC of native human skin. This may render the HSEs more permeable.

When examining the transition from a hexagonal to a liquid phase, this transition occurs at a lower temperature in the investigated HSEs compared to human SC. Previous studies show that a reduced free fatty acid content cannot explain this phenomenon, since a reduction in the free fatty acid level increases the temperature at which a liquid phase is formed [50]. However, a reduced chain length

of the free fatty acids or the presence of unsaturated chains may contribute to the decrease in transition temperature [48].

Optimization of the barrier properties of HSEs

The presented results show that the increased permeability of the investigated HSEs is likely caused by an increased conformational disordering of the lipids compared to the lipids in human SC. Furthermore, we hypothesize that a higher number of lipid lamellae between the cells may also reduce the SC barrier function. Whether the pronounced hexagonal packing also plays a role is not clear yet, but will be subject of future research. The change in lipid profile compared to native human SC indicates that the lipid metabolism in these HSEs differs from native human skin. Each HSE is generated under the same incubator conditions, but still shows (slight) differences in their lipid composition. Additionally, our in-house HSEs have an improved SC lipid composition and lamellar organization compared to the commercially available HSEs studied so far [14]. Taken together this implies that factors such as substrates used for HSE generation, culture media or other culture conditions can have an influence on the lipid metabolism in the viable epidermis resulting in changes in the SC barrier properties. Over the past years modulation of e.g. culture media or culture environment have improved epidermal development and consequently the lipid profiles and SC barrier formation of HSEs [15, 25, 35, 51]. Ponec *et al.* [35] showed that addition of vitamin C to the culture medium improved the lamellar body formation, extrusion and thus the intercellular lipid lamellae formation. The epidermal lipid metabolism was altered and resulted in an increased amount of ceramides AS and AP and detection of ceramide AH in the SC. Further optimization of culture media and culture conditions may lead to further improvements in the epidermal lipid metabolism in HSEs, such as an increase in the free fatty acid synthesis to induce the orthorhombic packing. Additionally, improvements made in the culture conditions may also enhance epidermal homeostasis, which in turn may lead to improved SC barrier properties.

Further optimization of the SC barrier properties of the presented HSEs, to resemble the SC barrier properties of native human skin more closely, will be subject of future research.

ACKNOWLEDGEMENTS

We would like to thank Dr. Maria Ponec for suggestions and discussions during our meetings and for proof reading the article. The Netherlands organization for Scientific Research is acknowledged for providing beam time at the ESRF in Grenoble. We would also like to thank Dr. W. Bras and co-workers for assistance at the ESRF. We are grateful to Evonik (Essen, Germany) for providing the ceramides. This research was financially supported by the Dutch Technology Foundation (STW; grant no. 7503).

REFERENCES

1. Brusselaers, N., Pirayesh, A., Hoeksema, H., Richters, C.D., Verbelen, J., Beele, H., Blot, S.I. and Monstrey, S. Skin replacement in burn wounds. J Trauma **68,** 490, 2010.
2. Shakespeare, P.G. The role of skin substitutes in the treatment of burn injuries. Clin Dermatol **23,** 413, 2005.
3. Supp, D.M. and Boyce, S.T. Engineered skin substitutes: practices and potentials. Clin Dermatol **23,** 403, 2005.
4. Alepee, N., Tornier, C., Robert, C., Amsellem, C., Roux, M.H., Doucet, O., Pachot, J., Meloni, M. and de Brugerolle de Fraissinette, A. A catch-up validation study on reconstructed human epidermis (SkinEthic RHE) for full replacement of the Draize skin irritation test. Toxicol In Vitro **24,** 257, 2009.
5. Gibbs, S. In vitro irritation models and immune reactions. Skin Pharmacol Physiol **22,** 103, 2009.
6. Netzlaff, F., Lehr, C.M., Wertz, P.W. and Schaefer, U.F. The human epidermis models EpiSkin, SkinEthic and EpiDerm: an evaluation of morphology and their suitability for testing phototoxicity, irritancy, corrosivity, and substance transport. Eur J Pharm Biopharm **60,** 167, 2005.
7. El Ghalbzouri, A., Siamari, R., Willemze, R. and Ponec, M. Leiden reconstructed human epidermal model as a tool for the evaluation of the skin corrosion and irritation potential according to the ECVAM guidelines. Toxicol In Vitro **22,** 1311, 2008.
8. Carlson, M.W., Alt-Holland, A., Egles, C. and Garlick, J.A. Three-dimensional tissue models of normal and diseased skin. Curr Protoc Cell Biol **Chapter 19,** Unit 19 9, 2008.
9. Engelhart, K., El Hindi, T., Biesalski, H.K. and Pfitzner, I. In vitro reproduction of clinical hallmarks of eczematous dermatitis in organotypic skin models. Arch Dermatol Res **297,** 1, 2005.
10. Garlick, J.A. Engineering skin to study human disease--tissue models for cancer biology and wound repair. Adv Biochem Eng Biotechnol **103,** 207, 2007.
11. Mildner, M., Jin, J., Eckhart, L., Kezic, S., Gruber, F., Barresi, C., Stremnitzer, C., Buchberger, M., Mlitz, V., Ballaun, C., Sterniczky, B., Fodinger, D. and Tschachler, E. Knockdown of filaggrin impairs diffusion barrier function and increases UV sensitivity in a human skin model. J Invest Dermatol **130,** 2286, 2010.
12. Boelsma, E., Gibbs, S., Faller, C. and Ponec, M. Characterization and comparison of reconstructed skin models: morphological and immunohistochemical evaluation. Acta Derm Venereol **80,** 82, 2000.

13. El-Ghalbzouri, A., Gibbs, S., Lamme, E., Van Blitterswijk, C.A. and Ponec, M. Effect of fibroblasts on epidermal regeneration. Br J Dermatol **147,** 230, 2002.
14. Ponec, M., Boelsma, E., Weerheim, A., Mulder, A., Bouwstra, J. and Mommaas, M. Lipid and ultrastructural characterization of reconstructed skin models. Int J Pharm **203,** 211, 2000.
15. El Ghalbzouri, A., Lamme, E. and Ponec, M. Crucial role of fibroblasts in regulating epidermal morphogenesis. Cell Tissue Res **310,** 189, 2002.
16. Boehnke, K., Mirancea, N., Pavesio, A., Fusenig, N.E., Boukamp, P. and Stark, H.J. Effects of fibroblasts and microenvironment on epidermal regeneration and tissue function in long-term skin equivalents. Eur J Cell Biol **86,** 731, 2007.
17. Stark, H.J., Boehnke, K., Mirancea, N., Willhauck, M.J., Pavesio, A., Fusenig, N.E. and Boukamp, P. Epidermal homeostasis in long-term scaffold-enforced skin equivalents. J Investig Dermatol Symp Proc **11,** 93, 2006.
18. Bouwstra, J., Pilgram, G., Gooris, G., Koerten, H. and Ponec, M. New aspects of the skin barrier organization. Skin Pharmacol Appl Skin Physiol **14 Suppl 1,** 52, 2001.
19. White, S.H., Mirejovsky, D. and King, G.I. Structure of lamellar lipid domains and corneocyte envelopes of murine stratum corneum. An X-ray diffraction study. Biochemistry **27,** 3725, 1988.
20. McIntosh, T.J., Stewart, M.E. and Downing, D.T. X-ray diffraction analysis of isolated skin lipids: reconstitution of intercellular lipid domains. Biochemistry **35,** 3649, 1996.
21. Bouwstra, J.A., Gooris, G.S., van der Spek, J.A. and Bras, W. Structural investigations of human stratum corneum by small-angle X-ray scattering. J Invest Dermatol **97,** 1005, 1991.
22. Bouwstra, J.A., Gooris, G.S., Dubbelaar, F.E. and Ponec, M. Phase behavior of lipid mixtures based on human ceramides: coexistence of crystalline and liquid phases. J Lipid Res **42,** 1759, 2001.
23. Goldsmith, L.A. and Baden, H.P. Uniquely oriented epidermal lipid. Nature **225,** 1052, 1970.
24. Damien, F. and Boncheva, M. The extent of orthorhombic lipid phases in the stratum corneum determines the barrier efficiency of human skin in vivo. J Invest Dermatol **130,** 611, 2010.
25. Batheja, P., Song, Y., Wertz, P. and Michniak-Kohn, B. Effects of growth conditions on the barrier properties of a human skin equivalent. Pharm Res **26,** 1689, 2009.
26. Schmook, F.P., Meingassner, J.G. and Billich, A. Comparison of human skin or epidermis models with human and animal skin in in-vitro percutaneous absorption. Int J Pharm **215,** 51, 2001.

27. Netzlaff, F., Kaca, M., Bock, U., Haltner-Ukomadu, E., Meiers, P., Lehr, C.M. and Schaefer, U.F. Permeability of the reconstructed human epidermis model Episkin in comparison to various human skin preparations. Eur J Pharm Biopharm **66,** 127, 2007.
28. Schafer-Korting, M., Bock, U., Diembeck, W., Dusing, H.J., Gamer, A., Haltner-Ukomadu, E., Hoffmann, C., Kaca, M., Kamp, H., Kersen, S., Kietzmann, M., Korting, H.C., Krachter, H.U., Lehr, C.M., Liebsch, M., Mehling, A., Muller-Goymann, C., Netzlaff, F., Niedorf, F., Rubbelke, M.K., Schafer, U., Schmidt, E., Schreiber, S., Spielmann, H., Vuia, A. and Weimer, M. The use of reconstructed human epidermis for skin absorption testing: Results of the validation study. Altern Lab Anim **36,** 161, 2008.
29. Asbill, C., Kim, N., El-Kattan, A., Creek, K., Wertz, P. and Michniak, B. Evaluation of a human bio-engineered skin equivalent for drug permeation studies. Pharm Res **17,** 1092, 2000.
30. Ackermann, K., Borgia, S.L., Korting, H.C., Mewes, K.R. and Schafer-Korting, M. The Phenion full-thickness skin model for percutaneous absorption testing. Skin Pharmacol Physiol **23,** 105, 2010.
31. Marjukka Suhonen, T., Pasonen-Seppanen, S., Kirjavainen, M., Tammi, M., Tammi, R. and Urtti, A. Epidermal cell culture model derived from rat keratinocytes with permeability characteristics comparable to human cadaver skin. Eur J Pharm Sci **20,** 107, 2003.
32. Zghoul, N., Fuchs, R., Lehr, C.M. and Schaefer, U.F. Reconstructed skin equivalents for assessing percutaneous drug absorption from pharmaceutical formulations. Altex **18,** 103, 2001.
33. Gibbs, S., Vicanova, J., Bouwstra, J., Valstar, D., Kempenaar, J. and Ponec, M. Culture of reconstructed epidermis in a defined medium at 33 degrees C shows a delayed epidermal maturation, prolonged lifespan and improved stratum corneum. Arch Dermatol Res **289,** 585, 1997.
34. Kennedy, A.H., Golden, G.M., Gay, C.L., Guy, R.H., Francoeur, M.L. and Mak, V.H. Stratum corneum lipids of human epidermal keratinocyte air-liquid cultures: implications for barrier function. Pharm Res **13,** 1162, 1996.
35. Ponec, M., Weerheim, A., Kempenaar, J., Mulder, A., Gooris, G.S., Bouwstra, J. and Mommaas, A.M. The formation of competent barrier lipids in reconstructed human epidermis requires the presence of vitamin C. J Invest Dermatol **109,** 348, 1997.
36. Pappinen, S., Hermansson, M., Kuntsche, J., Somerharju, P., Wertz, P., Urtti, A. and Suhonen, M. Comparison of rat epidermal keratinocyte organotypic culture (ROC) with

intact human skin: lipid composition and thermal phase behavior of the stratum corneum. Biochim Biophys Acta **1778,** 824, 2008.

37. Bouwstra, J.A., Gooris, G.S., Weerheim, A., Kempenaar, J. and Ponec, M. Characterization of stratum corneum structure in reconstructed epidermis by X-ray diffraction. J Lipid Res **36,** 496, 1995.
38. El Ghalbzouri, A., Commandeur, S., Rietveld, M.H., Mulder, A.A. and Willemze, R. Replacement of animal-derived collagen matrix by human fibroblast-derived dermal matrix for human skin equivalent products. Biomaterials **30,** 71, 2009.
39. Bouwstra, J.A., Groenink, H.W., Kempenaar, J.A., Romeijn, S.G. and Ponec, M. Water distribution and natural moisturizer factor content in human skin equivalents are regulated by environmental relative humidity. J Invest Dermatol **128,** 378, 2008.
40. Thakoersing, V.S., Ponec, M. and Bouwstra, J.A. Generation of human skin equivalents under submerged conditions-mimicking the in utero environment. Tissue Eng Part A **16,** 1433, 2009.
41. De Jager, M., Groenink, W., Bielsa i Guivernau, R., Andersson, E., Angelova, N., Ponec, M. and Bouwstra, J. A novel in vitro percutaneous penetration model: evaluation of barrier properties with p-aminobenzoic acid and two of its derivatives. Pharm Res **23,** 951, 2006.
42. Bligh, E.G. and Dyer, W.J. A rapid method of total lipid extraction and purification. Can J Biochem Physiol **37,** 911, 1959.
43. Motta, S., Monti, M., Sesana, S., Caputo, R., Carelli, S. and Ghidoni, R. Ceramide composition of the psoriatic scale. Biochim Biophys Acta **1182,** 147, 1993.
44. Masukawa, Y., Narita, H., Shimizu, E., Kondo, N., Sugai, Y., Oba, T., Homma, R., Ishikawa, J., Takagi, Y., Kitahara, T., Takema, Y. and Kita, K. Characterization of overall ceramide species in human stratum corneum. J Lipid Res **49,** 1466, 2008.
45. Caussin, J., Gooris, G.S., Janssens, M. and Bouwstra, J.A. Lipid organization in human and porcine stratum corneum differs widely, while lipid mixtures with porcine ceramides model human stratum corneum lipid organization very closely. Biochim Biophys Acta **1778,** 1472, 2008.
46. Cheng, T., Tjabringa, G.S., van Vlijmen-Willems, I.M., Hitomi, K., van Erp, P.E., Schalkwijk, J. and Zeeuwen, P.L. The cystatin M/E-controlled pathway of skin barrier formation: expression of its key components in psoriasis and atopic dermatitis. Br J Dermatol **161,** 253, 2009.
47. Bouwstra, J.A., Gooris, G.S., Bras, W. and Talsma, H. Small angle X-ray scattering: possibilities and limitations in characterization of vesicles. Chem Phys Lipids **64,** 83, 1993.

48. Janssens, M., Gooris, G.S. and Bouwstra, J.A. Infrared spectroscopy studies of mixtures prepared with synthetic ceramides varying in head group architecture: coexistence of liquid and crystalline phases. Biochim Biophys Acta **1788,** 732, 2009.
49. Groen, D., Poole, D.S., Gooris, G.S. and Bouwstra, J.A. Is an orthorhombic lateral packing and a proper lamellar organization important for the skin barrier function? Biochim Biophys Acta 2010.
50. Gooris, G.S. and Bouwstra, J.A. Infrared spectroscopic study of stratum corneum model membranes prepared from human ceramides, cholesterol, and fatty acids. Biophys J **92,** 2785, 2007.
51. Mak, V.H., Cumpstone, M.B., Kennedy, A.H., Harmon, C.S., Guy, R.H. and Potts, R.O. Barrier function of human keratinocyte cultures grown at the air-liquid interface. J Invest Dermatol **96,** 323, 1991.